NICMOS Status

A. B. Schultz,[1] D. Calzetti, S. Arribas,[2] T. Böker,[2] M. Dickinson, S. Malhotra

Space Telescope Science Institute, 3700 San Martin Drive, Baltimore, MD 21218

L. Mazzuca

NASA's Goddard Space Flight Center, Greenbelt, MD 20771

B. Mobasher,[2] K. Noll, E. Roye, M. Sosey, T. Wiklind,[2] and C. Xu

Space Telescope Science Institute, 3700 San Martin Drive, Baltimore, MD 21218

Abstract. The Near Infrared Camera and Multi-Object Spectrometer (NICMOS) is operational with improved scientific performance relative to the Cycle 7 & 7N. It has been performing routine science observations since June 12, 2002. The NICMOS detectors are operating at a higher temperature (77.1 ± 0.08 K (3σ)) than during Cycles 7 & 7N ($\sim$62 K). The instrument temperature has been fairly stable (±0.08 K at the detector), which allows stable optics and instrument's characteristics. Due to the higher operating temperature, the detector QE is higher, which results in $\sim$0.23 magnitude fainter detection limit in H for a 3σ detection of a point source in a 3,000 second integration.

1. Introduction

The Near Infrared Camera and Multi-Object Spectrometer (NICMOS) was installed on the *Hubble Space Telescope* (*HST*) in February 1997 during the Second *HST* Servicing Mission (SM2). The on-orbit life time of NICMOS was shortened due to a thermal short. The nitrogen ice cryogen was exhausted on January 4, 1999, and data taking was suspended on January 11, 1999. The NICMOS detectors warmed up to temperatures around 260 K and were not available for scientific observations for about three years. A mechanical cooler, the NICMOS Cooling System (NCS), using a reverse-Brayton cycle (Cheng et al. 1998) was installed on March 8, 2002 during the *HST* Servicing Mission 3B (SM3B). The NCS activation was on March 18, 2002, followed shortly by the start of the NICMOS cool down. Subsequently, a set point temperature resulting in a detector temperature of 77.1 K was reached, and NICMOS data taking resumed.

The NICMOS has three infrared cameras (NIC1, NIC2, NIC3) with different focal ratios (f/80, f/45.7, f/17.2). The NIC1 PSF is critically sampled at 1.0 μm, the NIC2 PSF is critically sampled at 1.75 μm, and the NIC3 PSF is under sampled. Camera operations are independent and non-confocal. The three cameras have adjacent, but not spatially contiguous, fields-of-view (FOVs). Each camera has a 256×256 pixel HgCdTe focal plane array (NICMOS 3 detector architecture). With the dewar "anomaly," the detectors were moved forward toward the dewar face plate. This resulted in non-confocal imaging at the detectors. However, NIC1 and NIC2 can successfully be used in parallel to each other

---

[1]Science Programs, Computer Sciences Corporation

[2]On assignment from the Space Telescope Division of the European Space Agency (ESA)

at an intermediate focus position for most applications. The focus interface for NIC3 is beyond the adjustable range of the Pupil Alignment Mechanism (PAM). However, NIC3 can still be used for science observations at the best available focus as the slight defocus relative to optimal focus induces only a modest (∼15%) reduction of the PSF peak energy. The characteristics of the NICMOS cameras after the installation of NCS are presented in Table 1. More details about the new capabilities of NICMOS can be found in the *NICMOS Instrument Handbook for Cycle 12* (Malhotra et al. 2002).

Table 1.   Characteristics of NICMOS Cameras. The read noise is measured per read pair, the difference of two reads. The dark current is the linear signal remaining after removing the amp-glow and shading contribution from the total "dark" signal. The DQE values (fraction of incident photons detected) for post-NCS temperature of 77.1 K scaled from the ground-based values.

Characteristics	Camera 1	Camera 2	Camera 3
Pixel size	$0.043''$	$0.075''$	$0.2''$
Field of View	$11'' \times 11''$	$19.2'' \times 19.2''$	$51.2'' \times 51.2''$
read-noise	$\sim$30 e$^-$/pixel	$\sim$30 e$^-$/pixel	$\sim$30 e$^-$/pixel
dark current	0.145 e$^-$/sec/pixel	0.110 e$^-$/sec/pixel	0.202 e$^-$/sec/pixel
ADGAIN	5.4 e$^-$/DN	5.4 e$^-$/DN	6.5 e$^-$/DN
DQE (1.6 μm)	0.426	0.442	0.414

NICMOS provides direct infrared imaging in broad, medium, and narrow-band filters from 0.8 to 2.5 μm as well as three special observational modes; i.e., coronagraphic imaging, broad-band imaging polarimetry, and slit-less grism spectroscopy. These special NICMOS capabilities enable fundamental investigation into the nature of a wide variety of objects. Accompanying papers describe in detail each of these modes.

2.   NICMOS Cooling System (NCS)

The NICMOS Cooling System (NCS) consists of three major subsystems: a cryocooler which provides the mechanical cooling; a Capillary Pumped Loop (CPL) which transports the heat dissipated by the cryocooler to an external radiator; and a circulation loop which transports heat from the inside of the NICMOS dewar to the cryocooler via a heat exchanger. Cold neon gas is circulated to cool the detectors. The NCS was activated on March 18, 2002, and reached the operational detector temperature of 77.1 K four weeks later. The time line of the NICMOS detector cool down is presented in Figure 1.

A number of test programs were executed to verify the stability and repeatability of the NCS control law. Results to date indicate that the NCS has good control of the temperature and that there is a margin in the compressor speed to compensate for extra heat due to changes in spacecraft attitude, operation of the NICMOS and other science instruments in the Aft Shroud, and any changes due to seasonal conditions. An in-depth discussion of the NICMOS cool down can be found in the accompanying paper Böker et al. (2003).

3.   NICMOS Optical Stability

The optimal focus for each NICMOS camera was determined on a regular basis during Cycles 7 & 7N with the last of the pre-NCS focus measurements performed on January 4, 1999 (Suchkov et al. 1998). These results can be found on the NICMOS web page (http://www.stsci.edu/hst/nicmos/performance/focus). Images of the star cluster
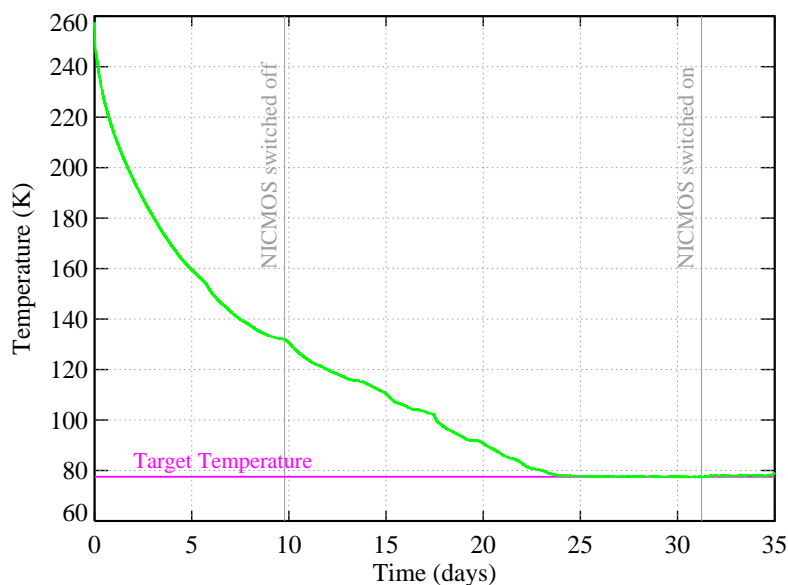
Figure 1. Time line of the NICMOS detector cool down.

NGC3603 (NIC/CAL program 8977) were obtained on May 3, 2002 to determine the locations of the NICMOS detectors with respect to the *HST* f/24 input beam. The data were independently analyzed using recovery of Zernike polynomial coefficients by phase retrieval and minimization of PSF core flux density dispersal by encircled energy. Comparisons made between phase retrieval and encircled energy measurements are in good agreement.

Results from the analysis indicated that the PAM positions, that affect best foci at the detectors, appeared to have moved marginally in the negative direction for NIC1 (PAM1) and NIC2 (PAM2) and in the positive direction for NIC3 (PAM3). The movement of NIC3 is towards its best focus. Thus, NIC3 focus is somewhat better than during Cycles 7 & 7N. The new PAM positions for all three cameras were uplinked to the telescope on May 9, 2002 together with the new intermediate NIC1 & NIC2 (PAMI) focus. No focus adjustments were implemented for NIC3 as the camera's optimal focus is located beyond the physical range of the PAM. No change to the coronagraphic focus (PAMC) was recommended at that time. The pre-NCS and current PAM positions are presented in Table 2. A monitor program, executed monthly for the first six months of Cycle 11 and bi-monthly afterwards, shows that the camera foci are relatively stable with a maximum excursion of ~0.5 mm of PAM movement from the default set points. A plot of the post-NCS focus history compared to the focus history for Cycles 7 & 7N is presented in Figure 2. Details about the focus determination can be found in the accompanying paper by Roye and Schultz (2003).

Table 2. The recommended nominal focus positions in mm of PAM motion. No breathing correction has been applied.

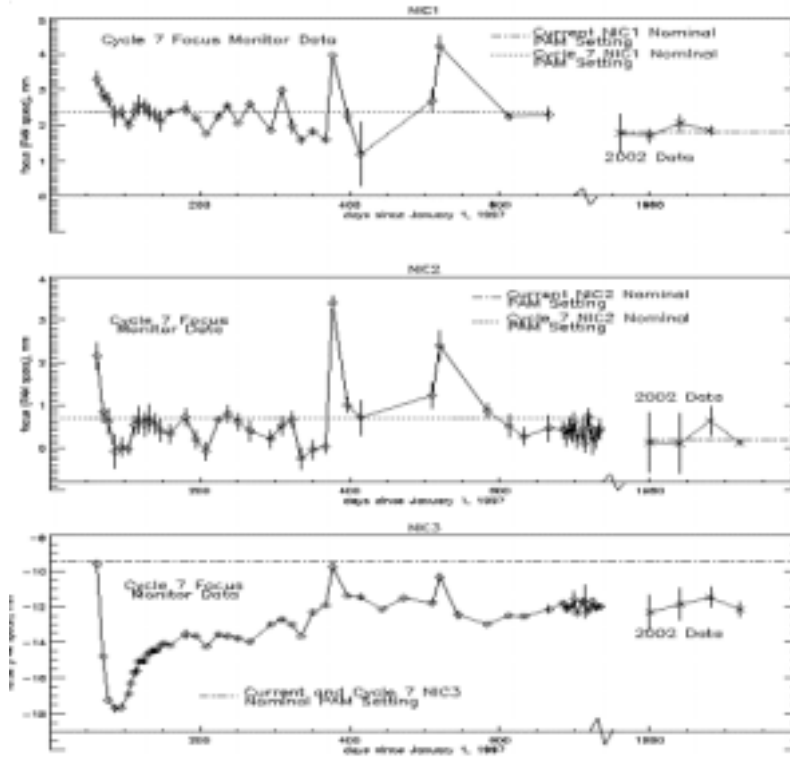| PAM1	PAM2	PAM3	PAMI	PAMC	Date
2.36	0.69	−9.50	1.75	2.69	pre-NCS
1.90	0.20	−9.50	1.22	2.69	post-NCS

Figure 2.   Post-NCS NICMOS focus history results compared to Cycles 7 & 7N. The *x*-axis represents the number of days since January 1, 1997 and *y*-axis represents the position of the PAM in mm.

A small amount of coma, observed in the post-NCS NICMOS and essentially absent in the Cycles 7 & 7N observations, has been corrected. The absence of such coma in the pre-NCS observations implies that a small amount of induced differential shear has occurred since January 1999. The presence of a small amount of coma did not affect the determination of the "best focus" by either of the two employed analysis methods discussed above. Coma corrections were determined separately for all three cameras. A set of data called a "tilt grid" was obtained which is a series of images taken at a variety of PAM tilt positions around the default position. New optimal PAM tilt setting for NIC1 were uplinked to *HST* on May 16, 2002. The correction successfully alleviated the observed NIC1 coma. New settings for NIC2 were uplinked on September 29, 2002, successfully alleviating all coma. No update was required for NIC3. Figure 3 presents the NIC1 and NIC2 PSFs before and after PAM tilt correction for coma. The NIC3 PSF is also shown for comparison. Details about the coma determination can be found in the accompanying paper Roye and Schultz (2003).

4.   Sensitivity Limits

The sensitivity of the NICMOS detectors is checked during each *HST* observing cycle by observing standard stars in each filter, the solar analog P330E and the white dwarf G19-B2B. In addition, a photometric monitor program is executed regularly during each cycle
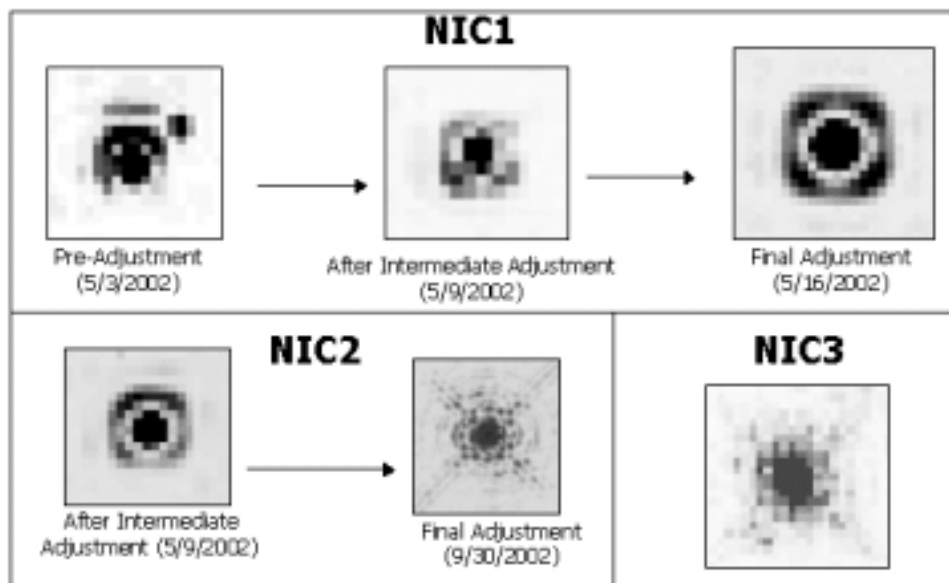
Figure 3.   NIC1 and NIC2 PSFs before and after PAM tilt correction for coma. NIC3 PSF is shown for comparison.

to observe standard stars in a selection of filters. These observations are used to determine the NICMOS photometric calibration and to determine the photometric stability of all three NICMOS detectors. The Cycles 7 & 7N photometric calibration data showed that the absolute photometry is accurate to 6% (1-σ uncertainty), and the temporal and spatial relative photometry is within 2% as well.

A check of the NICMOS photometric calibration was performed during June 2002 (SM3/NIC 8986). The solar analog P330E was observed in all three cameras with every broad, medium, and narrow band filters. Preliminary data reduction indicates an increase in the post-NCS photometric sensitivity of 20–70% depending on wavelength; this is consistent with the observed increase of the camera's DQE due to the higher operating temperature (see accompanying paper by Böker et al. 2003). Figure 4 shows the ratio of post-NCS photometric calibration to the Cycle 7 calibration. Further details about the photometric calibration can be found in the accompanying paper by Dickinson et al. (2003). The higher sensitivity can be quantified as a ~0.23 mag fainter 3 σ detection limit at H for a faint source with 3,000 sec exposure time. The new sensitivity limits are presented in Table 3 below.

Table 3.   NICMOS Sensitivity Limits. Cycle 11 magnitude limits to achieve S/N = 3 in 3600 sec for point source (80% encircled energy). AB magnitudes are at the standard NICMOS filter bands, where AB magnitudes are defined as $AB = -2.5 \log(F(\nu)) - 48.57$.

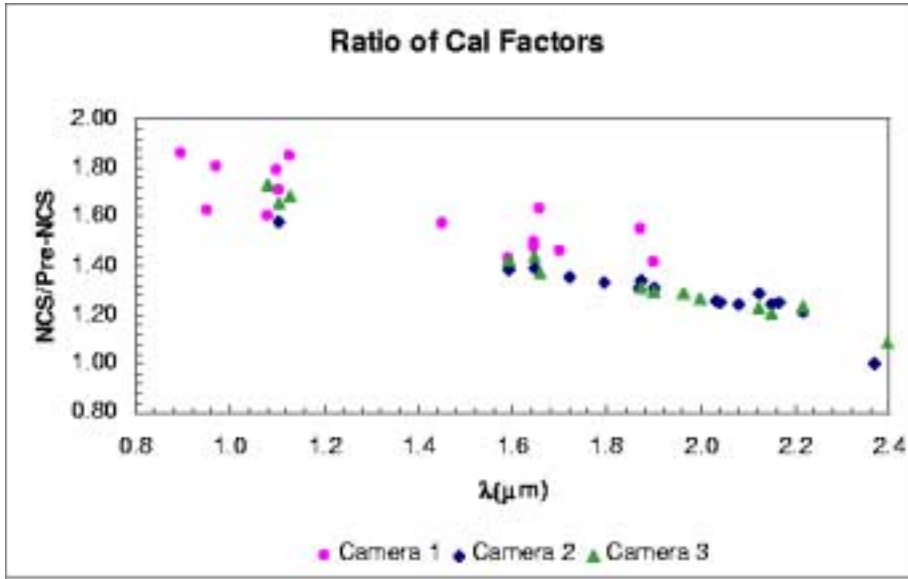|	NIC1	NIC2	NIC3
J_{AB}	24.6	25.2	25.2
H_{AB}	24.1	24.6	24.7
K_{AB}	—	21.8	21.4

Figure 4.   Post-NCS photometric calibration ratioed against Cycle 7 calibration.

5.   NICMOS Pipeline and User Tools

A suite of software tools have been developed to help the NICMOS observer calibrate, reduce, analyze, and to determine the quality of his data. Some of these tools are old favorites, while others are relatively new since Cycles 7 & 7N. Most importantly for those submitting Cycle 12 proposals is the updated *Exposure Time Calculator* (ETC). The ETC is set for the Cycle 11 operating temperature of 77.1 K. And for those retrieving NICMOS observations from the *HST* Archive, *On-The-Fly-Reprocessing* (OTFR) is now implemented for all NICMOS data retrieved from the Archive. Of note are two tools to create "Temperature Dependent Darks" and "Temperature Dependent Flat fields and Color Dependent Flats."

A summary of all available NICMOS software tools useful for data reduction and analysis along with a short discussion on the most recent updates to the calibration pipeline software (CALNICA and CALNICB) can be found in the accompanying paper by Sosey (2003).

An "old" problem with NICMOS observations is the persistence (residual image) induced by cosmic rays from passages through the South Atlantic Anomaly (SAA). In order to help alleviate the problem, the following steps have been taken:

1. Pairs of ACCUM darks are obtained with each camera after SAA passages to provide an "imprint" of the persistence image (post-SAA darks).

2. Four new keywords have been added to the headers of the science data (SAA_EXIT, SAA_TIME, SAA_DARK, SAACRMAP). The filenames of the post-SAA darks closest in time to the respective observation are written into the header keywords.

Finally, a persistence-removal method using the post-SAA darks is currently being investigated, together with the feasibility of an "automatic" routine to alleviate the persistence in science images.

Table 4.   The NICMOS Cycle 11 Calibration Goals

Calibration	Accuracy
Dark current and shading	4-5% on MULTIACCUM sequences
Flat fields	1% broad band, 3% narrow-band
Photometry	6% absolute, 2% relative and stability
PSF and Focus	1 mm
Astrometry	0.5% plate scale, $0.1''$ to FGS frame
Coronagraphic PSF	$0.013''$ in positing in hole
Grism wavelength calibration	0.005 μm
Grism photometric calibration	~30% absolute and relative
Polarimetry	1%
NIC3 intrapixel sensitivity	1-5%
High S/N capability character	S/N~10,000

6.   NICMOS Calibration Plan

A recalibration of the NICMOS primary capabilities has been initiated following the installation of the NCS and the subsequent cool down of the detectors. The NICMOS Cycle 11 calibration activities cover a period of 13 months. They complement the SMOV3B and the Cycle 10 interim calibration programs. These activities pursue the following major objectives: i) to monitor detector properties, ii) to provide data to test the model for generating darks, iii) to provide high S/N flat fields; iv) to investigate the intra-pixel sensitivity effects for NIC2 and NIC3, and v) to calibrate the three special observing modes; i.e., coronagraphy, polarimetry, and grism spectroscopy. Table 4 presents a list of the Cycle 11 calibration goals. Further details about the NICMOS Cycle 11 Calibration Plan can be found in the accompanying paper by Arribas et al. (2003).

References

Arribas, S., et al. 2003, this volume, 263

Böker, T., et al. 2003, this volume, 222

Cheng, E. S., Smith, R. C., Jedrichm N. M., Gibbon, J. A., Cottingham, D. A., Swift, W. L., & Dame, R. E. 1998, SPIE Proc., 3356, 1149

Dickinson, M., et al. 2003, this volume, 232

Hines, D. C., Schmidt, G. D., & Schneider, G. 2000, PASP, 112, 983

Malhotra, S., et al. 2002, *NICMOS Instrument Handbook for Cycle 12, Version 5.0*, (Baltimore: STScI) url: http://www.stsci.edu/hst/nicmos

Mazzuca, L. & Hines, D. C. 1999, "User's Guide to Polarimetric Imaging Tools," *Instrument Science Report* NICMOS-99-004 (Baltimore: STScI)

Roye, E. and Schultz, A. 2003, this volume, 267

Sosey, M. 2003, this volume, 275

Suchkov, A., Bergeron, L., & Galas, G. 1998, "NICMOS Focus Monitoring," *Instrument Science Report* NICMOS-98-004 (Baltimore: STScI)